

## 5. TURBIDITE FREQUENCY AND COMPOSITION IN THE DISTAL PART OF THE BAHAMAS TRANSECT<sup>1</sup>

Karin H. Bernet,<sup>2,4</sup> Gregor P. Eberli,<sup>2</sup> and Adrian Gilli<sup>3</sup>

### ABSTRACT

The lower slope and toe-of-slope sediments of the western flank of the Great Bahama Bank (Sites 1003 and 1007) are characterized by an intercalation of turbidites and periplatform ooze. In general, turbidites form up to 12% of the total mass of the sedimentary column. Based primarily on data from the Bahamas, it has been postulated that steep-sided carbonate platforms shed most of their sediments into the basin during sea-level highstands when the platforms are flooded. This highstand shedding is assumed to be less pronounced along platforms with a ramp-like depositional profile where sediment production is not restricted to sea-level highstand. Miocene to Pliocene sediments recovered in five drill holes during Leg 166 at the western margin of the Great Bahama Bank reveal that turbidite distribution follows a complex pattern that is dependent on several factors such as sedimentation rates, sea-level changes, and slope morphology.

To identify the depositional sequences in the cores, the depths of seismic-sequence boundaries were used. The distribution of turbidites within sedimentary sequences varies strongly. Generally, turbidites are clustered at the upper and/or lower portions of the sequences indicating deposition of carbonate turbidites during both highstand and lowstand of sea level. Analyses of the Miocene turbidites show that (1) during high sea level, 60% of all turbidites were deposited at Site 1003 (309 out of 518 turbidites), while during low sea level, two thirds of all turbidites were deposited at Site 1007 (332 out of 486 turbidites); (2) the average thickness of highstand turbidites is 1.5 times higher than the average thickness of lowstand turbidites; and (3) the turbidites display slight differences in composition and sorting. In general, highstand turbidites are less sorted and contain an abundant amount of shallow-water constituents such as green algae, red algae, shallow-water benthic foraminifers (miliolids), and intraclasts. The lowstand turbidites are better sorted and contain abundant planktonic foraminifers and micrite.

To complicate matters, highstand and lowstand turbidites seem to be deposited at different locations on the slope. At the lower slope (Site 1003), more turbidites were deposited during highstands, while at the toe of the slope, turbidites were dominantly deposited during sea-level lowstands. The result is a slope section with laterally discontinuous turbidite lenses within periplatform ooze, which is controlled by the interplay of sea-level changes, sediment production, and platform morphology.

### INTRODUCTION

The origin of carbonate turbidites has been the subject of debate since the introduction of depositional models that are guided by sequence stratigraphy. Sequence stratigraphy has postulated that in siliciclastic depositional systems most sediment is shed into the deep basins during lowstands of sea level (Vail et al., 1977). Whether this principle is applicable to the carbonate depositional system is at the heart of the controversy. Scientists working with carbonates have presented evidence that carbonate depositional systems are 180° out of phase with siliciclastic systems. Carbonate platform rates of production are highest when the platform is flooded. During these times, more sediment is produced than can be accumulated on the platform top, and this excess sediment is exported into the adjacent basins (Supko, 1963; Kier and Pilkey, 1971; Lynts et al., 1973; Hana and Moore, 1979; Hine et al., 1981; Droxler et al., 1983; Boardman and Neuman, 1984; Schlager et al., 1994). The higher sedimentation rate may result in overloading of the slope and gravitational instability, which are major contributing factors in the generation of turbidity currents (Middleton and Hampton, 1976; Crevello and Schlager, 1980). Therefore, it is reasonable to expect a higher frequency of turbidity currents during times of high slope-to-basin sedimentation, which for isolated platforms appears to correlate with relative highstands of sea level (Mullins, 1983).

This highstand shedding of turbidites has been well documented in the Quaternary sections surrounding the Bahamas (Droxler et al., 1983; Droxler and Schlager, 1985; Reijmer et al., 1988; Glaser and Droxler, 1991). A similar pattern of deposition has been interpreted from ancient slope sections surrounding isolated platforms in the Triassic and the Cretaceous (Reijmer et al., 1991; Harris 1994; Vecsei and Sanders, 1997). In ancient deposits, analyses of turbidite shedding have commonly relied on the analysis of grain composition. In these methods, the turbidites containing more platform interior grains were assumed to be shed during sea-level highstand, while turbidites containing grains predominantly from the margin were shed in times of low sea level (Reijmer et al., 1991).

In this study we take advantage of the geometries seen on the seismic sections. Seismic-sequence boundaries that indicate sea-level falls were determined at the platform margin of the Great Bahama Bank using erosional features and onlap patterns (Eberli, Swart, Malone, et al., 1997). On Leg 166, five sites were drilled on the transect of the western flank of the Great Bahama Bank. The sedimentary sections drilled at these sites were correlated to a multichannel, high-resolution seismic section on which 17 third-order seismic-sequence boundaries were traced from the platform top down to the basin (Eberli, Swart, Malone, et al., 1997). The seismic and sedimentary data were used to define highstand and lowstand systems tracts within the sequences.

In this paper we show that turbidites are shed during both sea-level highstand and lowstand. In addition, our data indicate a shift of the depositional location with changing sea level. For example, in the Miocene, sea-level highstands produced a high turbidite frequency on the lower slope (Site 1003), whereas the turbidite deposits at the toe of the slope (Site 1007) were dominantly shed during sea-level lowstand. Our analyses also document a relative small amount of turbidites along the entire transect, which suggests that deposition from

<sup>1</sup>Swart, P.K., Eberli, G.P., Malone, M.J., and Sarg, J.F. (Eds.), 2000. *Proc. ODP, Sci. Results*, 166: College Station TX (Ocean Drilling Program).

<sup>2</sup>Rosenstiel School of Marine and Atmospheric Science, Comparative Sedimentology Laboratory, 4600 Rickenbacker Causeway, University of Miami, Miami FL 33149, USA.

<sup>3</sup>Geologisches Institut ETHZ, Sonneggstrasse 5, 8092 Zürich, Switzerland.

<sup>4</sup>Present address: Rottmannsbodenstrasse 133, CH - 4102 Binningen, Switzerland. [khbernet@pop.bluewin.ch](mailto:khbernet@pop.bluewin.ch)

turbidity currents is not a dominant process in exporting sediment to the deep-water areas.

### BACKGROUND

The Ocean Drilling Program (ODP) drilled seven sites along the prograding carbonate margin of the western Great Bahama Bank to document the sedimentary record of Neogene sea-level changes (Eberli, Swart, Malone, et al., 1997). Five of these sites cover the upper to lower slope, the toe of the slope, and the basin and represent a continuation of the proximal Bahamas Drilling Project (BDP) sites Unda and Clino, which were drilled on the platform top (Fig. 1). The depth of these sites ranges from 200 to 700 to 1300 mbsf. Four different facies characterize the sediment along the Bahamas Transect:

1. Calcareous nannofossil ooze with changing amounts of planktonic foraminifers or bioclasts,
2. Monotonous peloidal wackestone to packstone,
3. Redeposited carbonate sediments (mass gravity flow deposits), and
4. Siliciclastic sediments (mainly silt and/or clay).

Along this prograding carbonate margin, alternations consisting of more neritic and more pelagic carbonate sediments form the perennial background sedimentation into which the redeposited beds are intercalated. The facies and the distribution of the redeposited beds change from the slope to the basin. At the upper slope (Sites 1004 and 1005), the sedimentary packages contain bioclastic packstone to

wackestone, pelagic intervals, some siliciclastic layers, and organic material but very few redeposited beds (Eberli, Swart, Malone, et al., 1997). On the lower slope and at the toe of the slope (Sites 1003 and 1007), intercalations of carbonates with mass gravity flow deposits, such as turbidites, slumps, and debris flow units, are common. The position of these deposits shows that most mass gravity flows bypassed the upper slope and were deposited at the break of the slope. In the basin axis (Site 1006), a thick package of current deposits consists of small-scale alternations of more platform-derived material and more pelagic sediments similar to the background sedimentation on the slope but no turbidites (Eberli, Swart, Malone, et al., 1997).

### METHODS

In this study, we combined seismic-sequence stratigraphic information with the analysis of the calcareous turbidites to examine the relationship between turbidite frequency and sea-level fluctuations. This methodology differs from other studies in that the separation of sea-level highstand and lowstand is based strongly on the geometry seen on the seismic section and not on the indirect evidence such as grain composition.

### Sedimentary Sequence Analysis

Seismic-sequence boundaries were used to separate the cores into highstand and lowstand systems tracts. The depth of the seismic-sequence boundary was calculated through the time/depth conversion from the vertical seismic profile shot at each site. This conversion has

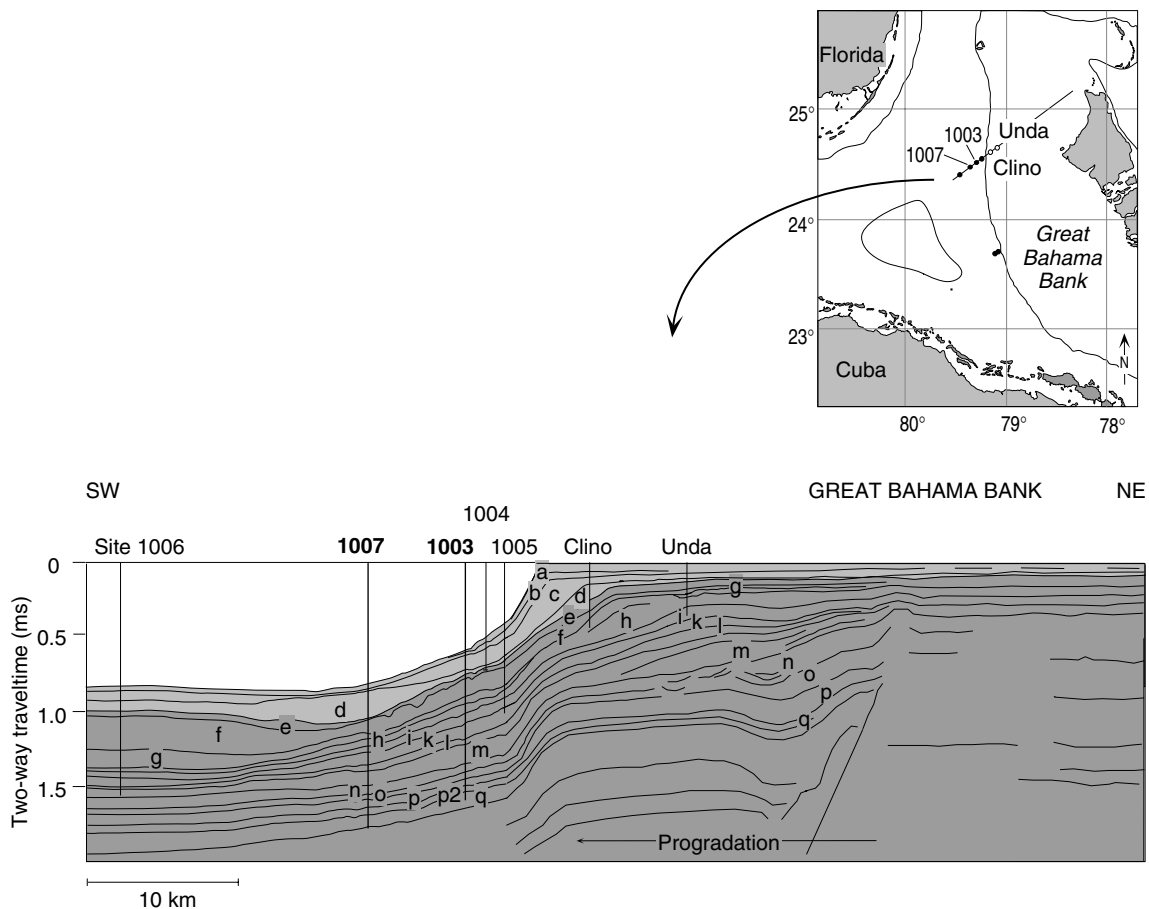


Figure 1. Schematic diagram of the Bahamas Transect showing the margin geometries, BDP boreholes Unda and Clino, and Leg 166 sites. Sites 1003 and 1007 are located at the lower slope and the toe of the slope, respectively. This prograding carbonate margin evolved from a low-angle, ramp-like geometry to a steep-sided (Sequences d-a) platform during the early Pliocene.

a resolution of 5–10 m maximum. The exact position of the sequence boundary in the core is determined by sedimentologic criteria within the interval given by the seismic resolution (Eberli, Swart, Malone, et al., 1997). In this study, the transgressive systems tract is included in the lowstand portion of the sequence. This can be justified by the fact that generally the platform was only flooded during highstands. To place the maximum flooding, or the turn-around from lowstand to highstand system tracts within each sequence, we relied on changes in texture together with mineralogy (low-Mg calcite [LMC], high-Mg calcite [HMC], aragonite, and quartz) and standard gamma-ray logs. This separation was based on the following evidence:

Supko (1963) and Boardman (1978) found that aragonite with a high strontium content originates on the bank top (from green algae, ooids, and inorganic precipitation), whereas pteropods show a low-strontium variety and represent planktonic aragonite. Droxler et al. (1983) document that 90% of the Bahamian aragonite in fine fraction is derived from a shallow-water source. Similarly, several authors assume a shallow-water source for HMC in the Bahamian troughs (Kier and Pilkey, 1971; Boardman, 1978; Droxler et al., 1983). Therefore, we assume that sections with high aragonite and HMC content, which are currently produced on the platform top, are indicative of deposits of high sea level when the platform is flooded.

In contrast, sections with increased LMC content and siliciclastic material probably represent lowstand system tracts for the following reasons: (1) Several authors showed that coccoliths and globigerinids, which predominantly occur in the open ocean, can account for nearly all the LMC (Kier and Pilkey, 1971; Boardman 1978; Droxler et al., 1983); (2) further, high contents of quartz, which appear whenever aragonite contents are low (Droxler et al., 1983), are likely to represent sea-level lowstand when the platform production is shut down and no aragonite or HMC are produced on the bank and exported into the basin. We acknowledge that diagenetic alteration of the mineralogic composition of the sediments may contribute to the difficulty of applying the mineralogic criteria but found no inconsistent behavior in our cores (Tables 1, 2).

A second criterion for separating lowstand from highstand systems tracts is taken from the gamma-ray log. Standard gamma-ray logs record the presence of potassium, thorium, and uranium present in potassium feldspars, micas, glauconite, and phosphate (Asquith and Gibson, 1982). Glauconite and phosphate are diagenetic minerals that precipitate from sea water in deeper parts of open platforms or nonrimmed margins (Scoffin, 1987). Uranium and potassium are present in green algae, certain corals (zoantharials and calcitic octocorals), pelecypods, gastropods, and arthropods found on hardground surfaces (Milliman et al., 1974). Hence, the natural gamma radiation increases at hardgrounds. Kenter et al. (in press) showed that in the proximal part of the transect at Unda and Clino, each sea-level cycle has an associated change in gamma radiation, and that the gamma-ray excursions also represent maximum flooding surfaces. The standard gamma-ray log can be correlated to the texture and lithology of the sediment and the mineralogy. Sequence k at Site 1003 (Fig. 2), for example, documents that the texture of the carbonate sediments changes

up-section from bioclastic wackestone to packstone, to peloidal packstone to grainstone with bioclasts, and is capped by a peloidal grainstone to rudstone with bioclasts. At the first increase in texture, the aragonite values decrease to zero and the amount of quartz increases dramatically. At the same depth, the standard gamma-ray log shows the highest peak underlain by two smaller but also dominant peaks. Based on a sudden appearance of peloids following the quartz peak and the low value of aragonite (Betzler et al., in press), we assume that the high excursion in gamma radiation that often coincides with clay layers represents the maximum flooding surface within the sequence. In such cases, the gamma-ray peaks are used to separate lowstand from highstand systems tracts. The separation of sea-level highstand vs. lowstand packages based on the above criteria enables us to assess the distribution of the turbidite composition and frequency within the individual sequences.

### Calibration of Turbidites to Log Data

The core recovery at Sites 1003 and 1007 was 55% and 73%, respectively. To reveal the total amount of turbidites and their thickness, we calibrated the sedimentary description to the log data (Fig. 3). Carbonate turbidites generally consist of coarser material than the sedimentary composition of the background sediments and, therefore, show differences in resistivity values. The Formation Micro-Scanner (FMS) records resistivity where highly resistive intervals are displayed in bright colors, and layers with low resistivity values are shown in dark colors. Thus, FMS images have been powerful in distinguishing turbidite deposits from background sediments (Williams and Pirmez, in press).

In high-recovery cores, we characterized the resistivity pattern of the FMS log and compared it to the turbidite deposits and surrounding sediment. Changes in texture in normally or inversely graded turbidite deposits were recognized as subtle color changes from bright to dark colors or from dark to bright colors. The strongest color contrast is represented by the sudden change from fine-grained background sediment to a coarse-grained turbidite layer. The resolution of the resistivity tool is, however, not high enough to record other sedimentary structures. For example, in the cores, the sediments showed parallel laminations that were rather difficult to recognize in the FMS images. This may also be related to Mullins' (1983) and Eberli's (1991) observation that complete Bouma sequences may or may not be present and that there appears to be a lateral segregation of top-cut-out turbidites in more proximal positions (Section 166-1003B-56X-1, 12–32 cm) and base-cut-out turbidites in more distal regions (Section 166-1007C-43R-3, 85–110 cm). In any rate, the FMS could be used to identify turbidite deposits that were not recorded in low-recovery sections. Nevertheless, we estimate that a certain number of turbidites was not detected by the FMS logs. One of the factors of "miss-measuring" the thickness may be related to the difficulties of recognizing the finer grained turbidites in the FMS images, because it is rather difficult to separate the top of a fining-upward turbidite sequence from the fine background sediment. Knowing these difficul-

**Table 1. Mineralogical composition of samples, Site 1003.**

Depth (mbsf)	Dolomite (%)	LMC (%)	HMC (%)	Aragonite (%)	Quartz (area)
0.41	0.0	9.0	25.5	57.6	0
3.41	0.0	3.9	8.7	80.2	0
6.41	0.0	5.6	7.3	80.1	0
7.41	0.0	4.6	6.1	81.9	0
8.91	0.0	5.3	5.9	81.8	0
10.41	0.0	6.8	7.1	79.3	0
11.91	0.0	18.1	67.4	8.5	1039
12.68	0.0	8.9	41.2	45.5	0
13.99	0.0	20.5	4.8	69.7	100
15.49	0.1	22.3	8.3	63.3	0

Note: LMC = low-Mg calcite, HMC = high-Mg calcite.

This is a sample of the table that appears on the volume CD-ROM.

**Table 2. Mineralogical composition of samples, Site 1007.**

Depth (mbsf)	Dolomite (%)	LMC (%)	HMC (%)	Aragonite (%)	Quartz (area)
1.9	0.0	20.2	26.7	41.2	1.3
4.9	0.3	51.4	6.2	34.7	0.0
7.9	0.0	28.6	19.4	46.0	0.0
11.4	0.0	58.4	7.4	26.1	0.4
14.4	0.4	14.0	4.1	76.8	0.0
17.4	0.6	23.7	6.9	64.1	0.0
20.9	0.3	22.6	6.4	65.7	0.0
23.9	0.0	18.1	3.6	72.9	0.0
30.4	0.0	10.5	2.5	81.7	0.0
33.4	0.2	21.1	1.6	70.5	0.0

Note: LMC = low-Mg calcite, HMC = high-Mg calcite.

This is a sample of the table that appears on the volume CD-ROM.

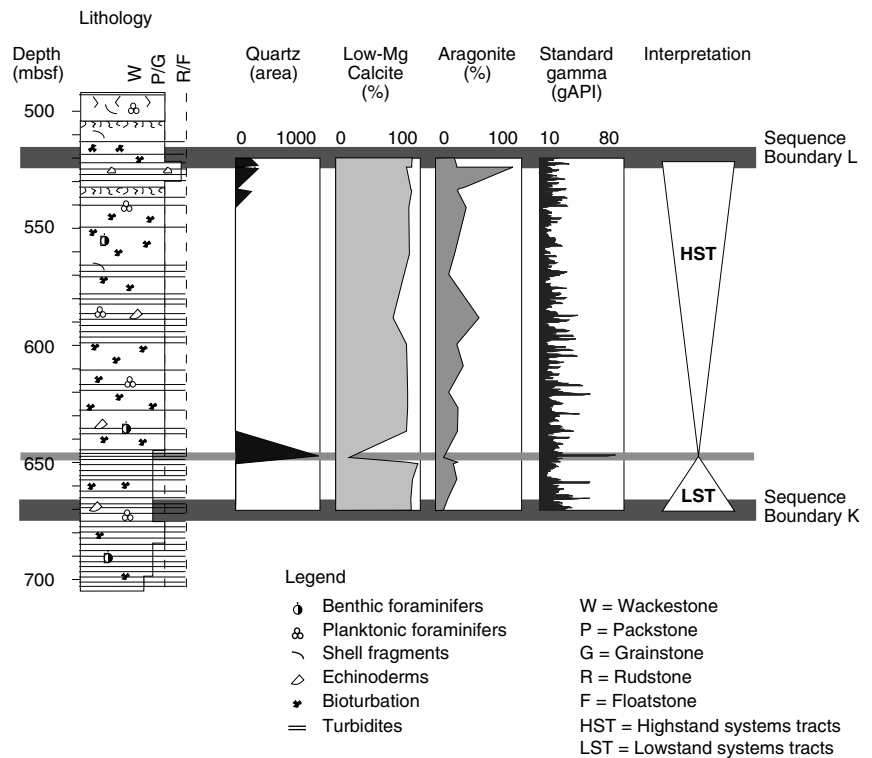


Figure 2. Cores were separated into highstand and lowstand system tracts using seismic-sequence boundaries to distinguish highstand from lowstand deposits, and texture, mineralogy (low-Mg calcite, aragonite, and quartz), and standard gamma-ray logs for placing the boundary between the lowstand and the highstand within each sequence. The transgressive system tract is included in the lowstand portion of the sequence. Note the gamma-ray peak coinciding with the quartz peak (here at Site 1003).

ties, we have to accept that the thickness and the actual number of turbidites in the sedimentary section exceeds the counted number and measured thickness of tabulated turbidites (confirmed by C. Betzler, pers. comm., 1998). We are confident, though, that the relative proportions of both the thickness and number of turbidites at the two sites are true, since the same methods were used for both sites.

We counted all the carbonate turbidites at Sites 1003 and 1007 and measured their thicknesses using the core description and/or the FMS log. The frequency of turbidite shedding was calculated in events per meter section and events per sedimentary sequence.

### Grain Composition

A total number of 241 samples were taken throughout the cores from Sites 1003 and 1007. The samples represent different events of turbidite shedding and background sediments in the Miocene and early Pliocene. We concentrated our compositional analyses on the Miocene. In each thin section, 300 points were counted to determine the compositional differences of turbidites and background sediments and to describe the compositional differences of highstand and lowstand deposits (Tables 3, 4). The term "background sediment" includes three out of four facies that characterize the sediment along the Bahamas Transect and represent initial sediment that has not been re-deposited, such as periplatform ooze, peloidal wackestone to packstone, and siliciclastic sediments. Grains were counted once or more, according to their size (volumetrical counting). The quantities of the characteristic carbonate grains have been analyzed and were assigned to point-count groups that characterize the different depositional settings of the platform margin, (i.e., lagoon, reef complex, and basin). Nonskeletal grains and embedding sediment were counted in separate groups (Table 5).

## RESULTS

### Turbidite Frequency and Thickness

The sediments at Site 1003 at the lower slope and Site 1007 at the toe of the slope of the western Great Bahama Bank contained a higher percentage of redeposited beds, namely turbidites and debris flows,

than the other sites; therefore, we concentrated our study on these two sites. Slump deposits have not been included here, although Betzler et al. (in press) showed that most slumps can be clearly related to the occurrence of turbidite depositional systems. Within the 1104 m of Neogene sediments at Site 1003 (Sequence Boundaries C to P2), 463 turbidites have been counted with a total thickness of 130.18 m, which represents only 12% of the total sediment thickness. The average turbidite thickness is 28 cm. The sedimentary sequence analyses allowed us to separate these sediments into 16 packages of lowstand and highstand systems tracts (Fig. 4). Sequence q is not included, because the bottom of the Neogene was not reached at Site 1003. A total of 309 turbidites (67%) were shed during high sea level covering a thickness of 77.24 m (59% of the entire turbidite volume). During low sea level, only 154 turbidites were shed (33%) with a total thickness of 52.94 m (41% of total volume) (Fig. 5).

The distribution of turbidite deposits varies greatly from one sedimentary sequence to another (Table 6). Most turbidites were deposited during the late Langhian, Seravillian, and to some extent the early Tortonian (middle Miocene). In the Burgidalian, early Langhian, late Tortonian, Piacenzian, and Pleistocene, only a few turbidites were deposited, whereas during the Messinian and Zanclean, no turbidites were recorded in the cores of the studied sites.

The sediments at the basinal Site 1007 were separated into only 14 packages, because Sequence Boundaries A and B were not recorded and Sequence Boundaries D and E merged (Fig. 6). Within the 1155 m of Neogene sediments, 541 turbidites were counted (Sequence Boundaries C through Q). These turbidites had a total thickness of 51.84 m, with an average turbidite thickness of 10 cm. Only 39% of all turbidites at this site were deposited during sea-level highstand, while 61% were shed during sea-level lowstand. The thickness of the highstand turbidite deposits, however, is 29.90 m, which represents 57% of the total volume (Fig. 5). As is the case with Site 1003, most of the turbidites were shed in the Seravillian (middle Miocene), followed by Burgidalian, late Langhian, early Tortonian, early Messinian, and early Pliocene. Only a few turbidites were recorded in the early Langhian, late Tortonian, and late Messinian. Compared to Site 1003, overall the lowstand turbidites were more abundant except in the late Langhian (Table 7).

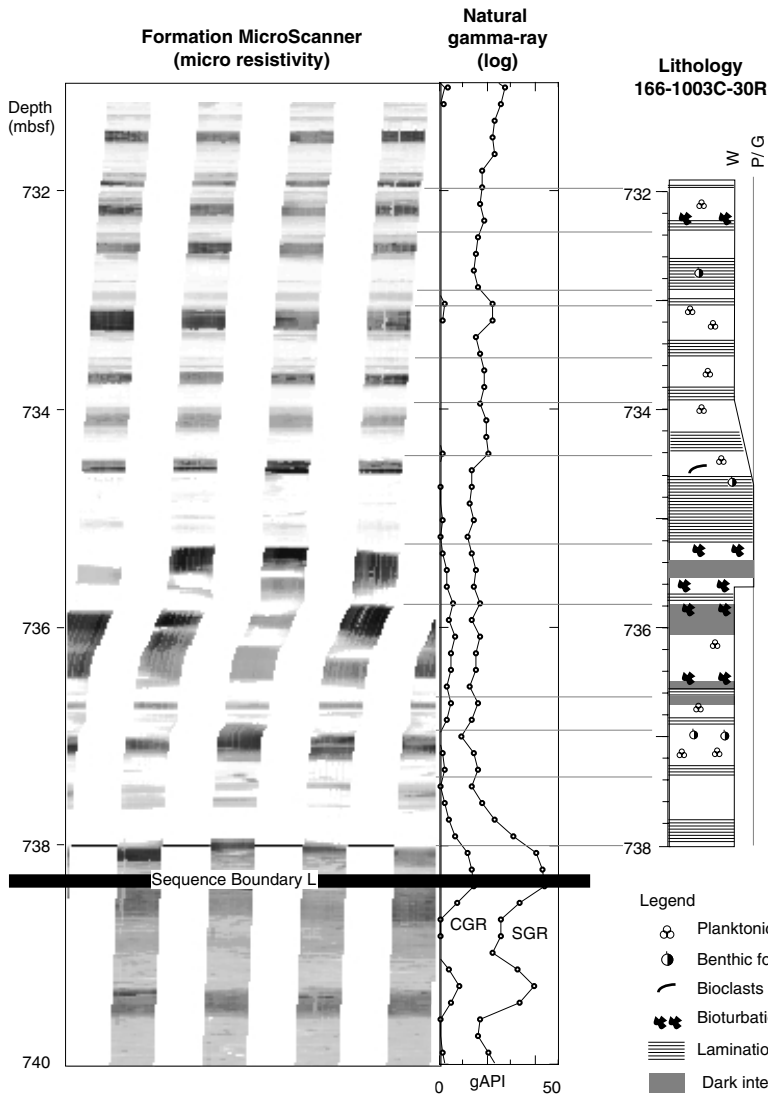


Figure 3: Part of the Formation MicroScanner (FMS) image and the lithology log (Site 1003) across a seismic-sequence boundary. The rhythmic high-frequency sedimentary cycles are interrupted by highly resistive beds (white color in the FMS image). The laminations in the lithology log were interpreted as turbidite deposits and were correlated to the resistive beds in the FMS. CGR = computed gamma ray, SGR = standard gamma ray. W = wackestone, P = packstone, G = grainstone.

Table 3. Composition of turbidite and background samples at Site 1003 determined from a point-count analysis.

Depth (mbsf)	Turbidite deposit (T)/ background sediment (B)		Highstand (H)/ lowstand (L)		Green algae					Benthic foraminifers			Planktonic foraminifers			Mollusks				Brachiopods				Micrite		Molds	
	T	B	H	L	Green algae	Red algae	Echinoderms	Benthic foraminifers	Rotalids	Buliminids	Nodosorids	Miliolids	Planktonic foraminifers	Mollusks	Brachiopods	Bioclasts	Lithoclasts	Intraclasts	Ooids	Micrite	Molds						
115.20	T	H	0	0.5	6	6	1	0	0	0	28	7	0	25	0	0	0	4	28	0							
138.71	B	L	0	1	0.3	5.6	0.5	0	0.1	0.2	18.6	0	0	4.4	0	0	0	0	38.6	26							
176.59	T	H	0	0.6	0.3	18	0.5	0.5	0.1	0.1	20.3	1.1	1.2	14.3	0	0	0	0.3	21.7	19.3							
176.76	B	H	0	0	1.6	9	8	1	0	0	18	0	1	3.3	0	0	0	0	25.3	34							
219.26	B	H	0	0	0	6.6	4.6	1.3	0.3	0	11.6	0.3	0	3.7	0	0	0	0	40.6	18.3							
219.66	B	H	0	0	0.3	6.3	5	0.7	0.7	0	7	0	0	2.3	0	0	0	0	32.6	31.3							
331.13	B	L	0	0	0.3	4.3	1.7	1.7	0.3	0	5.3	0	0.6	8	0	0	0	0	44.3	27.3							
349.10	B	L	0	0	2	3	0.7	2	0	0	4	0	0	6.3	0	0	0	0	38	30.3							
349.22	T	L	0	0.6	3	3.3	2	1.3	0	0	2.3	0	0	7	0	0	0	0.6	48.6	21.6							
408.15	B	H	0	0	0.5	8	0	0	0	0	7	10	0	22	0	0	2	0	47	0							

Note: The first Miocene sample was picked at a depth of 331.3 mbsf.

This is a sample of the table that appears on the volume CD-ROM.



**Sedimentary Sequences**

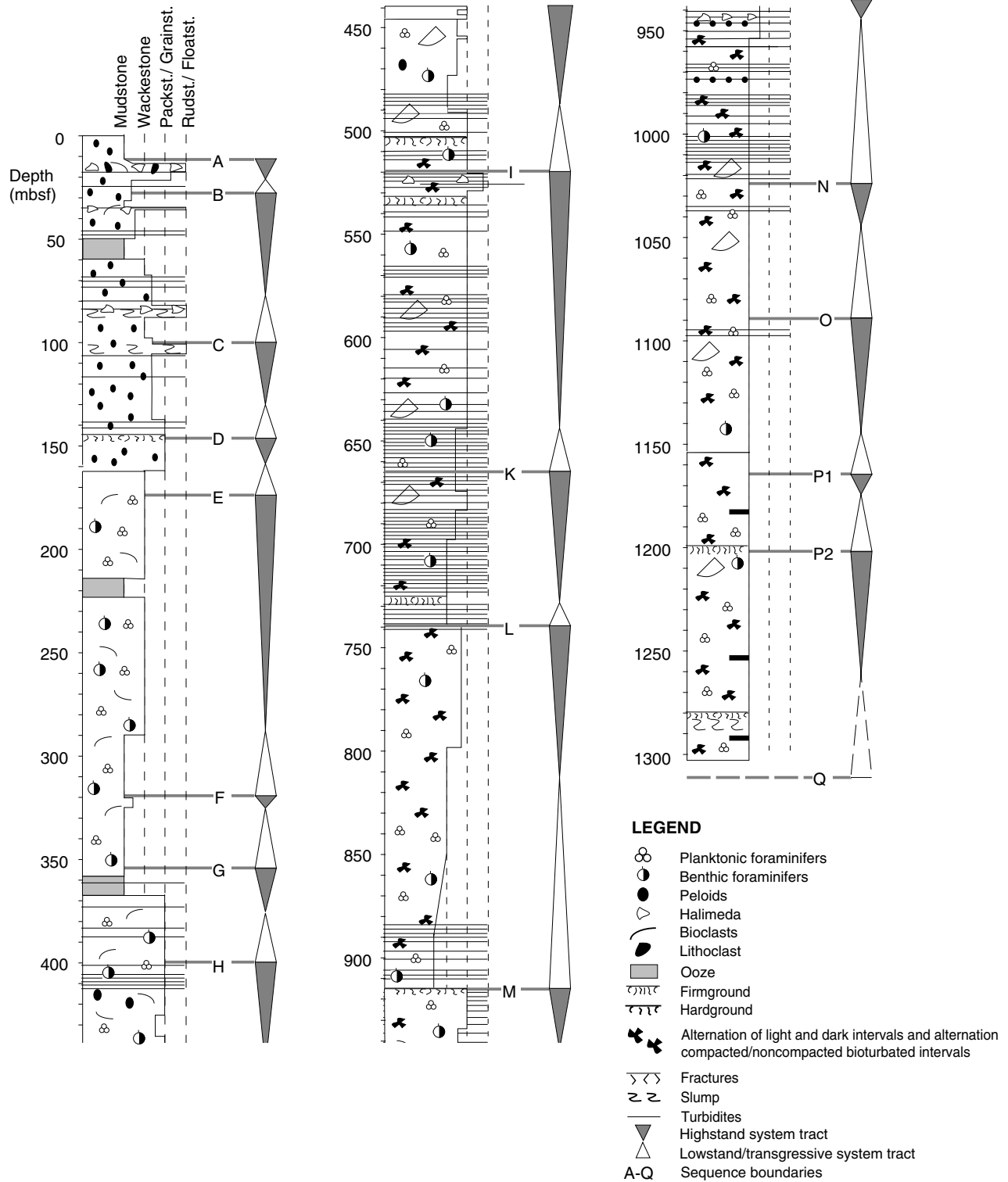


Figure 4. Lithologic description of the lower slope sediments of the Bahamas Transect (Site 1003) separated into highstand and lowstand systems tracts deposits. The lowstand systems tracts include the transgressive systems tracts. Seismic-sequence boundaries were used to separate the highstand systems tracts from the lowstand systems tracts. Within a sedimentary sequence, the number of turbidite events varies from 0 to over 100, and in general more turbidites were seen in highstand deposits.

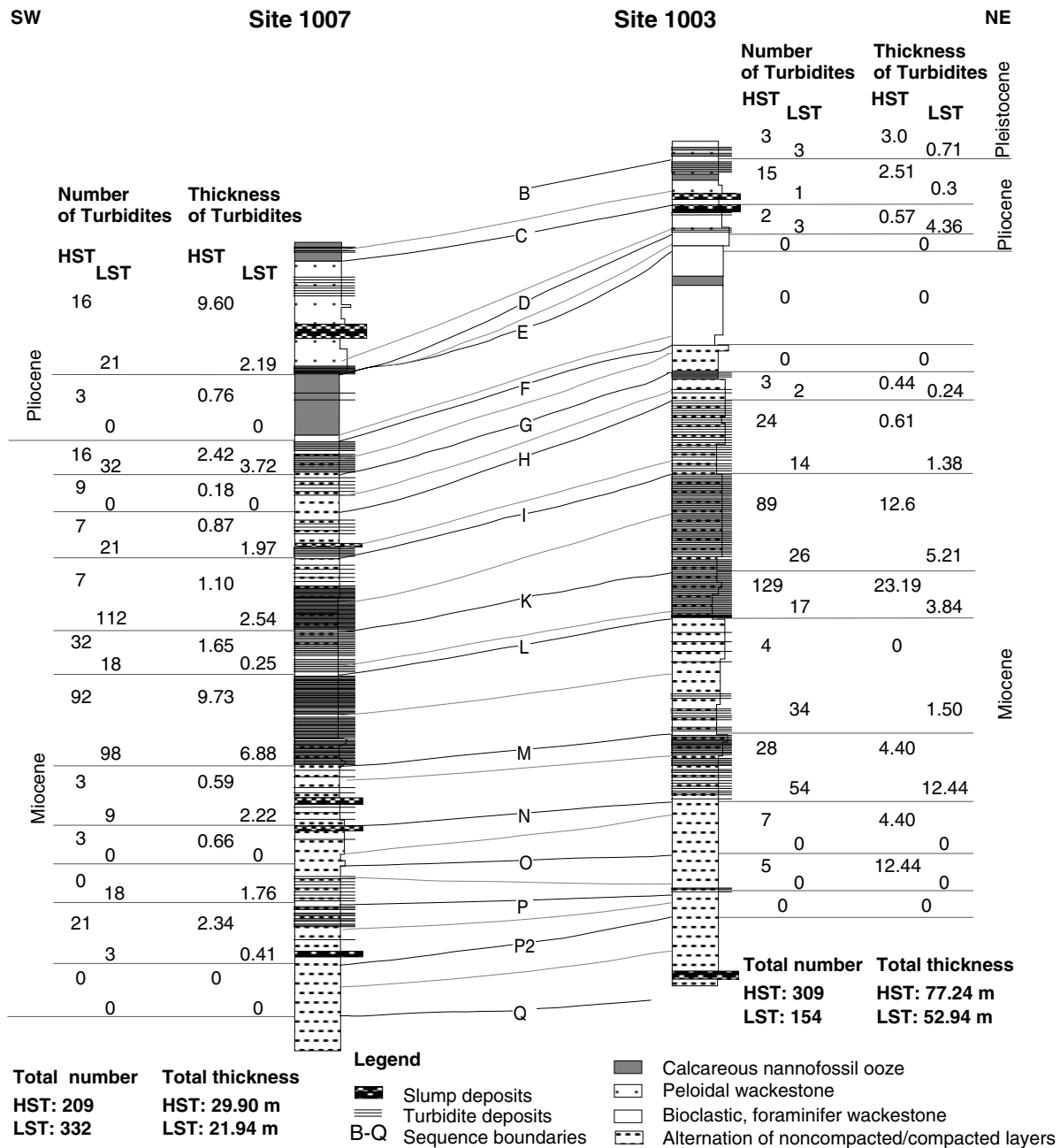


Figure 5. The distribution of turbidite deposits at Sites 1007 and 1003 displaying thickness and number of turbidites deposited during sea-level highstands. The dotted lines between the sequence boundaries represent the separation between lowstand and highstand systems tracts (LST, HST). Note that at Site 1003, the number of turbidites shed during sea-level highstand is twice as high as during lowstand in contrast to Site 1007, at which more turbidites were deposited during sea-level lowstand. The average thickness of turbidite layers is higher during high sea level.

mentation rates occur during sea-level highstands and produce thicker packages of turbidite deposits.

- The sedimentary composition is indicative of sea level. Turbidite deposits in general are characterized by shallow-water components, whereas the background sediment contains planktonic foraminifers and more fine-grained, muddy particles. Generally, the composition of turbidite and background sediments shows only slight changes from high to low sea level because the environmental change is limited on the ramp-like Miocene-Pliocene profile of the Great Bahama Bank. In fact, there are no significant differences in composition between highstand turbidites and lowstand turbidites in the Miocene. In some cases, the signal may even be reversed. Shallow-water

components indicative of sea-level lowstands at Site 1007 can be found in background sediments deposited during sea-level highstands at Site 1003 (Tables 8, 9). These compositional differences within the two sites indicate a shift of the carbonate production zone toward the basin during lowstands and toward the platform during highstands. This result indicates that the approach of using grain composition to determine highstand vs. lowstand turbidites in ancient turbidite systems will be best applicable along steep-sided platforms (Reijmer et al., 1991; Harris 1994; Vecsei and Sanders, 1997).

- The distribution of frequency and the location of turbidite deposition follow a complex pattern that is controlled by the interplay of sea-level changes and platform morphology. At the

lower slope (Site 1003), more turbidites are recorded in the Burgidalian and Langhian than at the toe of the slope (1007). In the Seravillian, however, both sites record a high occurrence of turbidites; but from the Tortonian to the Zanclian, more turbidites were deposited at Site 1007 (Tables 6, 7). This change in the deposition of turbidites indicates a downslope shift of the depocenter in the Tortonian, which may be related to the long-term sea-level lowstand in the late Miocene.

In several sequences, turbidites are deposited either during sea-level highstand or lowstand along the entire transect. Highstand shedding of turbidites occurs in Sequences h (upper Tortonian), l (middle Seravillian), and o (lower Langhian) at both Sites 1003 and 1007; while lowstand turbidites at both the lower slope and the toe of the slope are found in Sequences m and n (lower Seravillian and upper Langhian). This distribution does not seem to be correlated to relative sea-level changes. Sea level was very high during Sequences m and n. Therefore, these sequences should be dominated by highstand shedding of carbonates, but they are not. Similarly, the highstand shedding in Sequences c, h, l, and o cannot be explained by a relative high sea level, because sea level is relatively lower than during Sequences m and n. The data suggest a complicated distribution of frequency and location of deposition of turbidites along ramp-like carbonate platforms. About one fourth of the sequences show a change from highstand turbidites at the lower slope (Site 1003) to lowstand turbidites at the toe of the slope (Site 1007). Slight changes in slope angles and rates of sea-level changes seem to be responsible for these diverse patterns.

Our results seem to be inconsistent with the findings in Pleistocene sections of the Bahamas slopes where a clear highstand shedding of turbidites is documented (Droxler and Schlager, 1985; Reijmer et al., 1988). The difference can be explained by the change in platform morphology. During the Miocene and early Pliocene, the Great Bahama Bank developed from a ramp-like platform into the modern steep-sided platform. On the ramp-like platform, the carbonate production zone moved up and down the ramp with fluctuating sea level, resulting in a slight change in sediment production. Nevertheless, the thickness variations in highstand vs. lowstand turbidites confirm the assumption that the slope-to-basin sedimentation is higher during high sea level. As is the case with the production zone, the turbidite depocenters shift up and down the ramp with sea level; at sea-level highstand, the depocenter is further upslope than during sea-level lowstand. Furthermore, in such a setting, compositional differences are minor compared to steep-sided platforms where lowstand turbidites are dominated by eroded lithoclasts and abraded grains (Reijmer et al., 1988).

## CONCLUSION

In the Neogene, a larger number of carbonate turbidites were deposited during sea-level highstands than during lowstands in the distal position of the Bahamas Transect. Changing sea level influenced the location of turbidite deposition. During highstands, more turbidites were deposited at the lower slope; whereas during lowstands, more turbidites were deposited at the toe of the slope. This shift of turbidite deposition probably records the shift of the carbonate production zone with changing sea level. The generally slight compositional differences of the background sediments and turbidites at the two sites during highstands and lowstands show that on a ramp-like platform changing sea level may move the carbonate production zone upslope or downslope on such a platform geometry without major environmental changes.

The correlation of turbidite deposits within individual sequences documents three different shedding patterns: (1) sequences dominated by highstand shedding, (2) sequences dominated by lowstand shedding, and (3) sequences which show a change from highstand to

**Table 6. Distribution of turbidites shed within each lowstand or highstand systems tract in the Quarternary, Site 1003.**

Seismic sequence	Age (Ma)		HST turbidites	LST turbidites	Total turbidites
b	0.09-0.25	Pleistocene	3	3	6
c	0.250-01.2/1.6	Piacenzian	15	1	16
d	1.2/1.6-3.1	Piacenzian	3	2	5
e	3.1-3.8	Zanclian	0	0	0
f	3.8-5.6	Messinian	0	0	0
g	5.6-6.2/8.7	Messinian	0	0	0
h	6.2/8.7-9.0	Tortonian	3	2	5
i	9.0-10.6	Tortonian	24	14	38
k	10.6-12.2	Seravillian	89	26	115
l	12.2-12.7	Seravillian	129	17	146
m	12.7-13.6/15.1	Seravillian	4	34	38
n	13.6/15.1-15.9	Langhian	28	54	82
o	15.9-18.4	Langhian	7	0	7
p	18.4-19.4	Burgidalian	5	0	5

Note: HST = highstand systems tract, LST = lowstand systems tract. Most turbidites were shed in the middle Miocene. Note the high abundance of highstand turbidites in Sequences c, i, k, l, and n.

lowstand shedding. These patterns indicate a complex influence of sea level and platform morphology on turbidite frequency and deposition.

Because turbidites at Sites 1003 and 1007 represent only up to 12% of the sediment column, turbidity currents are not the dominant mechanism for depositing sediment on carbonate slopes. Therefore, the controversy related to highstand or lowstand shedding may only be partly solved by looking at turbidites.

## ACKNOWLEDGMENTS

We greatly appreciate the contribution and discussions of our shipboard colleagues in the sedimentary laboratory (ODP Leg 166). Special thanks to Christian Betzler for discussions and suggestions throughout the course of this study. We also express thanks to Mark Harris, Chris Kendall, and Rick Sarg for reviewing the manuscript and to Kelly Bergman for proofreading the English. The research was funded by a grant from JOI/USSAC (K.B.) and contributions from the Industrial Associates of the Comparative Sedimentology Laboratory at the University of Miami.

## REFERENCES

- Asquith, G.B., and Gibson, C.R., 1982. Basic well log analysis for geologists. *AAPG Methods Explor. Ser.*, 3:91-95.
- Betzler, C., Reijmer J.J.G., Bernet, K., Eberli, G.P., and Anselmetti, F.S., in press. Sedimentary patterns and geometries of the Bahamian outer carbonate ramp (Miocene and lower Pliocene, Great Bahama Bank). *Sedimentology*.
- Boardman, M.R., 1978. Holocene deposition in northwest Providence Channel, Bahamas: a geochemical approach [Ph.D. dissert.]. Univ. of North Carolina, Chapel Hill.
- Boardman, M.R., and Neumann, A.C., 1984. Sources of periplatform carbonates: Northwest Providence Channel, Bahamas. *J. Sediment. Petrol.*, 54:1110-1112.
- Crevello, P.D., and Schlager, W., 1980. Carbonate debris sheets and turbidites, Exuma Sound, Bahamas. *J. Sediment. Petrol.*, 50:1121-1148.
- Droxler, A.W., and Schlager, W., 1985. Glacial versus interglacial sedimentation rates and turbidite frequency in the Bahamas. *Geology*, 13:799-802.
- Droxler, A.W., Schlager, W., and Whallon, C.C., 1983. Quaternary aragonite cycles and oxygen-isotope record in Bahamian carbonate ooze. *Geology*, 11:235-239.
- Eberli, G.P., 1991. Calcareous turbidites and their relationship to sea-level fluctuations and tectonism. In Einsele, G., Ricken, W., and Seilacher, A. (Eds.), *Cycles and Events in Stratigraphy*: New York (Springer-Verlag), 340-359.
- Eberli, G.P., Swart, P.K., Malone, M.J., et al., 1997. *Proc. ODP, Init. Repts.*, 166: College Station, TX (Ocean Drilling Program).

- Glaser, K.S., and Droxler, A.W., 1991. High production and highstand shedding from deeply submerged carbonate banks, northern Nicaragua Rise. *J. Sediment. Petrol.*, 61:128–142.
- Hana, J.C., and Moore, C.H., 1979. Quaternary temporal framework of reef to basin sedimentation, Grand Cayman, B.W.I. *Geol. Soc. Am. Abstr. Progr.*, 11:438.
- Harris, M.T., 1994. The foreslope and toe-of-slope facies of the middle Triassic Latemar buildup (Dolomites, Northern Italy). *J. Sediment. Res.*, B64:132–145.
- Hine, A.C., Wilber, R.J., Bane, J.M., Neumann, A.C., and Lorenson, K.R., 1981. Offbank transport of carbonate sands along open, leeward bank margins: northern Bahamas. *Mar. Geol.*, 42:327–348.
- Kenter, J.A.M., Ginsburg, R.N., and Troelstra, S.R., in press. The western Great Bahama Bank: sea level-driven sedimentation patterns on the slope and margin. In Ginsburg, R.N. (Eds.), *SEPM Contrib. Sedimentol.*
- Kier, J.S., and Pilkey, O.H., 1971. The influence of sea level changes on sediment carbonate mineralogy, Tongue of the Ocean, Bahamas. *Mar. Geol.*, 11:189–200.
- Lynts, G.W., Judd, J.B., and Stehman, C.F., 1973. Late Pleistocene history of Tongue of the Ocean, Bahama. *Geol. Soc. Am. Bull.*, 84:2605–2684.
- Middleton, M.F., and Hampton, 1976. Subaqueous sedimentary transport and deposition by sediment gravity flows. In Stanley, D.J., and Swift, D.J.P. (Eds.), *Marine Sediment Transport and Environmental Management*: New York (Wiley), 197–218.
- Milliman, J.D., Mueller, G., and Foerstner, U., 1974. *Marine Carbonates*: New York (Springer-Verlag).
- Mullins, H.T., 1983. Modern carbonate slopes and basins of the Bahamas. In Cook, H.E. (Ed.), *Platform Margin and Deep-Water Carbonates*. Soc. Econ. Paleontol. Mineral., Short Course Notes, 12.
- Reijmer, J.J.G., Schlager, W., and Droxler, A.W., 1988. ODP Site 632: Pliocene-Pleistocene sedimentation cycles in a Bahamian basin. In Austin, J.A., Jr., Schlager, W., et al., *Proc. ODP, Sci. Results*, 101: College Station, TX (Ocean Drilling Program), 213–220.
- Reijmer, J.J.G., Ten Kate, W.G.H., Sprenger, A., and Schlager, W., 1991. Calciturbidite composition related to exposure and flooding of a carbonate platform (Triassic, Eastern Alps). *Sedimentology*, 38:1059–1074.
- Schlager, W., Reijmer, J., and Droxler, A.W., 1994. Highstand shedding of carbonate platforms, *J. Sediment. Res.*, B64:270–281.
- Scoffin, T.P., 1987. *Introduction to Carbonate Sediments and Rocks*: New York (Chapman and Hall).
- Supko, P.R., 1963. A quantitative X-ray diffraction method for the mineralogical analysis of carbonate sediments from Tongue of the Ocean [M.S. thesis]. Univ. of Miami, Coral Gables, FL.
- Vail, P.R., Mitchum, R.M., Jr., and Thompson, S., III, 1977. Seismic stratigraphy and global changes of sea level, Part 2. The depositional sequence as a basic unit for stratigraphic analysis. In Payton, C.E. (Ed.), *Seismic Stratigraphy: Applications to Hydrocarbon Exploration*. AAPG Mem., 26:53–62.
- Vecsei, A., and Sanders, D.G.K., 1997. Sea-level highstand and lowstand shedding related to shelf margin aggradation and emersion, Upper Eocene-Oligocene of Maiella carbonate platform, Italy. *Sediment. Geol.*, 112:219–234.
- Williams, T., and Pirmez, C., in press. FMS images from carbonates of the Bahama Bank Slope, ODP Leg 166: lithological identification and cyclostratigraphy. In Lovell, M., Williamson, G., and Harvey, P. (Eds.) *Borehole Images: Case Histories*. Geol. Soc. Spec. Publ. London.

**Date of initial receipt: 10 August 1998**

**Date of acceptance: 12 February 1999**

**Ms 166SR-112**

**Sedimentary Sequences**

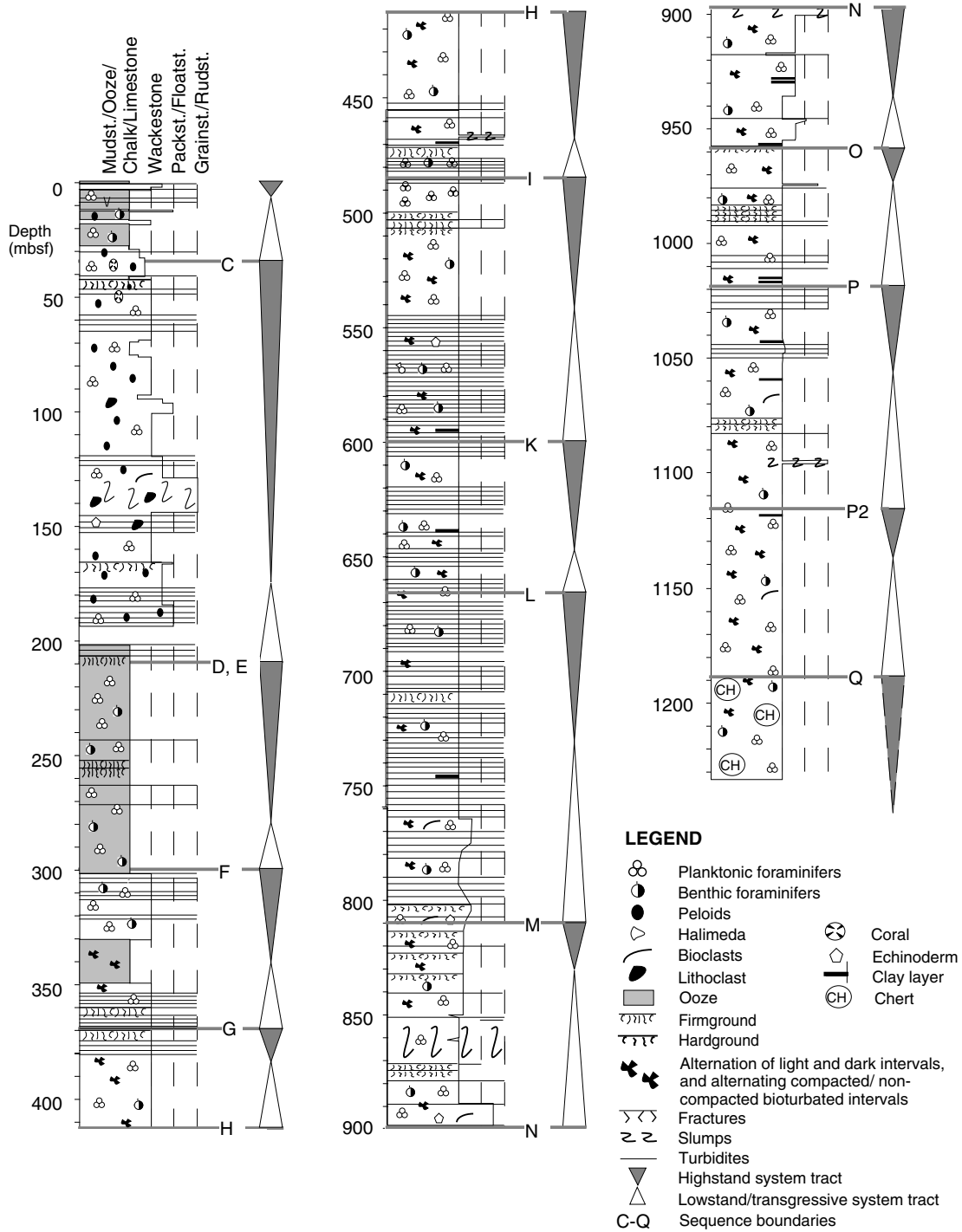


Figure 6. Lithologic description of the basal sediments of the Bahamas Transect (Site 1007) separated into highstand and lowstand systems tracts deposits. The transgressive systems tracts are included in the lowstand systems tracts. Seismic-sequence boundaries were used to separate the highstand systems tracts from the lowstand systems tracts. Within a sedimentary sequence, the number of turbidite events varies from 0 to 60. At Site 1007, more turbidites occur within the lowstand deposits.

**Table 7. Distribution of turbidites shed within each highstand or lowstand systems tract in the Pliocene/Miocene, Site 1007.**

Seismic sequence	Age (Ma)		HST turbidites	LST turbidites	Total turbidites
d	1.5/1.7-3.2/4.2	Zanclean	16	21	37
f	3.2/4.2-5.5/6.4	Messinian	3	0	3
g	5.5/6.4-8.8	Messinian	16	32	48
h	8.8-9.4	Tortonian	9	0	9
i	9.4-10.6	Tortonian	7	21	28
k	10.6-12.2	Seravillian	7	112	119
l	12.2-12.5	Seravillian	32	18	50
m	12.5-15.1	Seravillian	92	98	190
n	15.1-16.2/16.4	Langhian	3	9	12
o	2/16.4-18.2	Langhian	3	0	3
p	18.2-19.4	Burgidalian	0	18	18
p2	19.4-23.2	Burgidalian	21	3	24
q	23.2-23.7	Aquitanian	0	0	0

Notes: HST = highstand systems tract, LST = lowstand systems tract. Most turbidites were shed during the middle Miocene. The abundance of lowstand turbidites in Sequences d, g, i, k, m, and p is high.

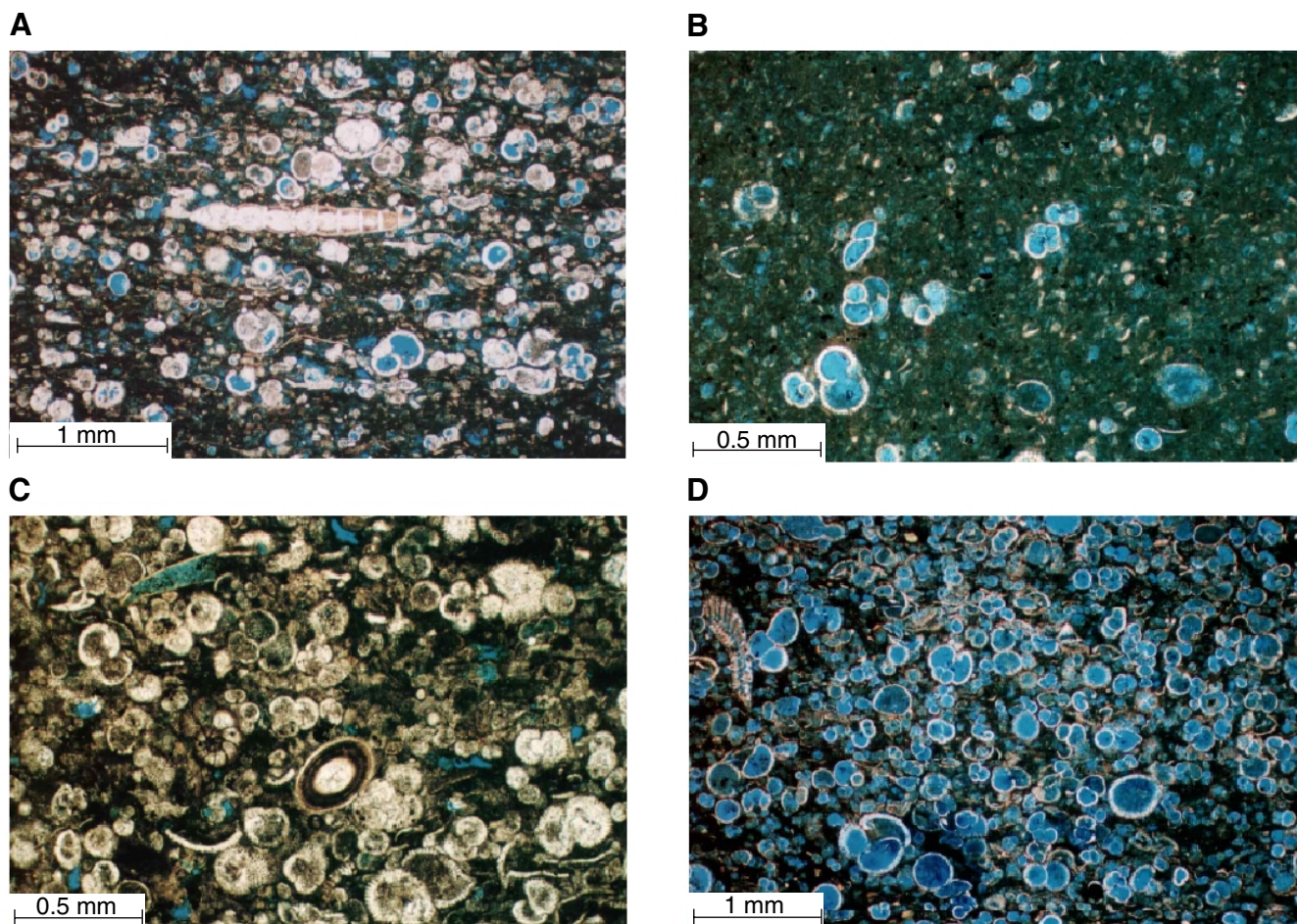


Figure 7. Typical microfacies from the Miocene interval documenting the differences of background sediments and turbidites at Sites 1003 and 1007. (A) The planktonic foraminifer wackestone to packstone rich in benthic foraminifers, and (B) the planktonic foraminifer wackestone with skeletal fragments represent the background sediments at Site 1003 and 1007, respectively. The turbidite deposits show (C) abundant neritic components (Site 1003), or (D) abundant planktonic and benthic foraminifers (Site 1007).

**Table 8. Statistical description of turbidite deposits and background sediments recovered at Site 1003.**

	Mean	SD	SE	Minimum	Maximum	Variance
<b>Background sediment:</b>						
Green algae	0.24	1.25	0.14	0	10	1.57
Red algae	0.22	0.94	0.10	0	8	0.88
Echinoderms	0.67	1.54	0.17	0	10	2.38
Rotaliids	0.64	1.19	0.13	0	8	1.41
Miliolids	0.05	0.21	0.02	0	1	0.04
Planktonic foraminifers	13.07	8.86	0.93	0	38	75.14
Mollusks	1.46	3.21	0.35	0	13	10.29
Bioclasts	22.45	15.85	1.71	1	66.3	251.22
Lithoclasts	0.67	2.48	0.27	0	20.3	6.17
Intraclasts	0.07	0.35	0.04	0	2.3	0.13
Ooids	1.44	3.66	0.39	0	22	13.40
Micrite	42.81	16.06	1.73	1.3	77	257.77
<b>Turbidite deposit:</b>						
Green algae	1.00	2.42	0.31	0	13	6.33
Red algae	0.79	1.47	0.19	0	7	2.32
Echinoderms	1.74	2.31	0.30	0	11	5.67
Rotaliids	0.51	0.8	0.10	0	3.3	0.61
Miliolids	0.25	0.51	0.07	0	2.3	0.14
Planktonic foraminifers	9.22	8.15	1.03	0.3	34	68.19
Mollusks	2.94	4.54	0.58	0	24	21.99
Bioclasts	22.04	16.92	2.15	1	63.6	296.72
Lithoclasts	0.97	2.14	0.27	0	12	4.83
Intraclasts	0.35	1.21	0.15	0	6	1.48
Ooids	5.01	10.44	1.33	0	74	115.4
Micrite	32.02	14.48	1.84	0	63.6	213.99

Note: SD = standard deviation, SE = standard error.

**Table 9. Statistical description of turbidite deposits and background sediments recovered at Site 1007.**

	Mean	SD	SE	Minimum	Maximum	Variance
<b>Background sediment:</b>						
Green algae	0.01	0.04	0.01	0	0.3	0.00
Red algae	0.10	0.35	0.05	0	1.5	0.12
Echinoderms	0.50	0.90	0.12	0	4	0.82
Rotaliids	0.42	0.64	0.09	0	3	0.41
Miliolids	0.03	0.12	0.02	0	0.7	0.01
Planktonic foraminifers	15.31	10.71	1.47	2.5	55	114.69
Mollusks	4.48	11.90	1.63	0	46	141.63
Bioclasts	18.72	11.65	1.60	1	48	135.61
Lithoclasts	0.08	0.33	0.05	0	2.3	0.11
Intraclasts	0.10	0.49	0.07	0	3	0.24
Ooids	0.80	3.01	0.41	0	21	9.05
Micrite	47.45	13.98	1.92	14	70.3	195.39
<b>Turbidite deposit:</b>						
Green algae	0.11	0.42	0.06	0	3	0.18
Red algae	0.39	0.84	0.11	0	3	0.71
Echinoderms	0.91	1.86	0.24	0	9.6	3.46
Rotaliids	0.50	0.78	0.10	0	4.6	0.61
Miliolids	0.04	0.12	0.02	0	0.6	0.01
Planktonic foraminifers	16.09	12.64	1.65	2	52	159.81
Mollusks	4.41	9.91	1.29	0	40	98.23
Bioclasts	22.77	12.93	1.68	0.5	56.6	167.27
Lithoclasts	0.42	1.75	0.23	0	13	3.06
Intraclasts	0.01	0.08	0.01	0	0.5	0.01
Ooids	1.64	3.3	0.43	0	20	10.91
Micrite	38.26	14.1	1.84	5	69	198.7

Note: SD = standard deviation, SE = standard error.

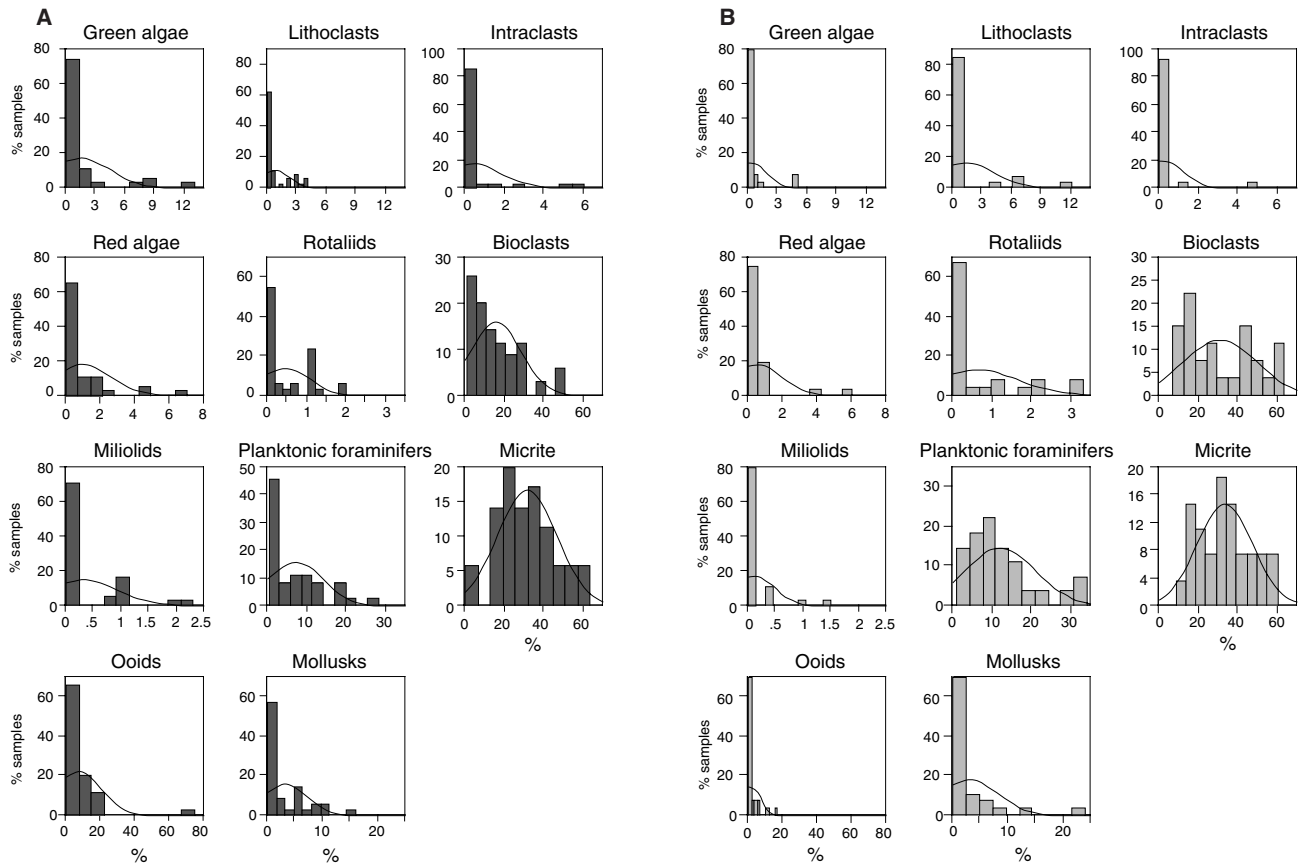


Figure 8. Comparison of the composition of turbidite sediments deposited during (A) sea-level highstand and (B) sea-level lowstand at the lower slope (Site 1003; Miocene). The sediments deposited during high sea level show a higher abundance of shallow-water components including green and red algae, ooids, and shallow-water benthic foraminifers (miliolids).

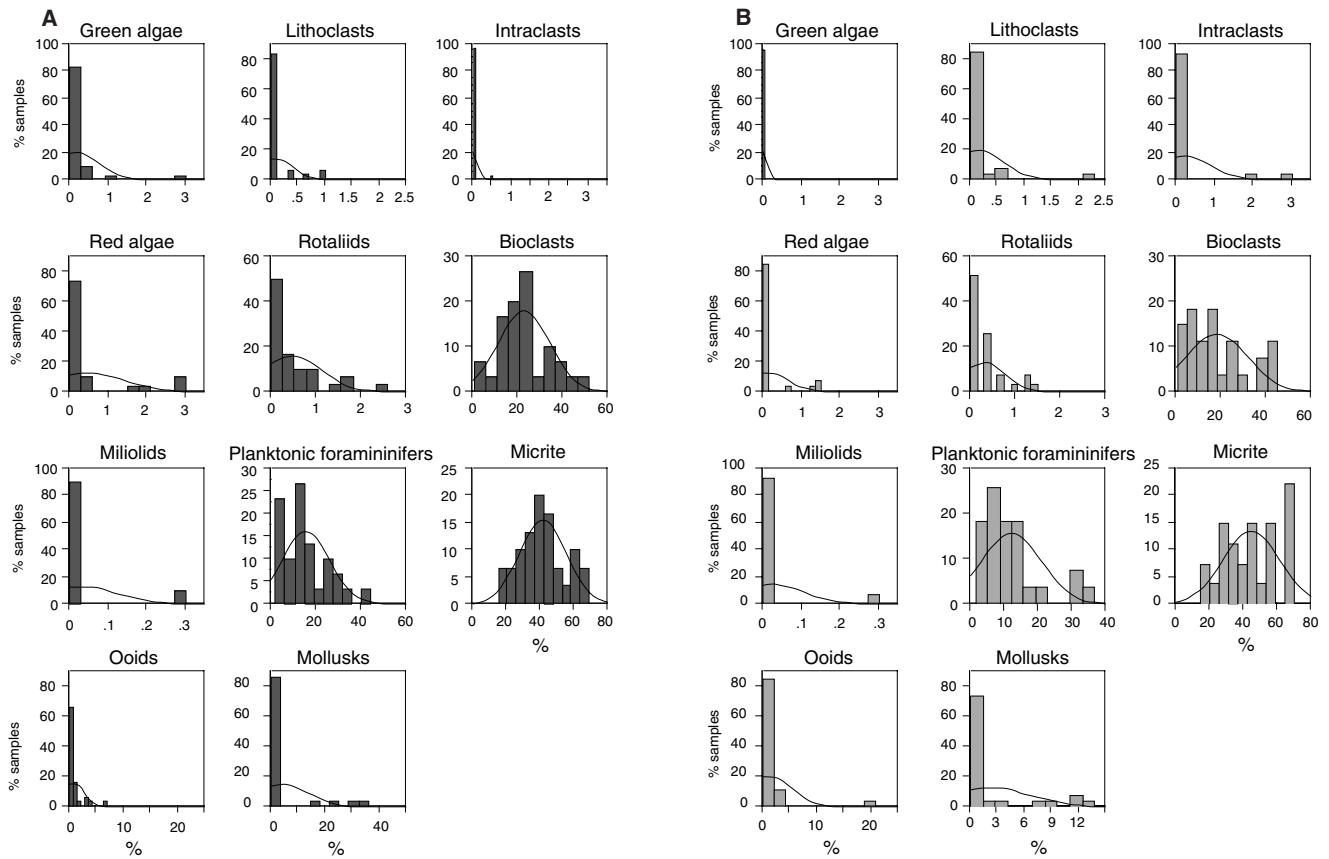


Figure 9. Distribution of turbidite constituents deposited during (A) sea-level highstand and (B) sea-level lowstand at Site 1007 (Miocene). Note the higher abundance of deep-water benthic foraminifers (rotaliids), bioclasts, green algae, and red algae during sea-level highstand. The lowstand constituents show a high abundance of ooids, lithoclasts, intraclasts, and mollusks.

Table 10. Statistical description of turbidite deposits shed during sea-level highstand and lowstand, Site 1003.

	Mean	SD	SE	Minimum	Maximum	Variance
<b>Highstand:</b>						
Green algae	1.41	2.96	0.50	0	13	8.79
Red algae	0.96	1.56	0.26	0	7	2.44
Echinoderms	1.83	2.46	0.42	0	11	6.07
Rotaliids	0.44	0.58	0.10	0	2	0.33
Miliolids	0.34	0.60	0.10	0	2.3	0.36
Planktonic foraminifers	7.08	6.91	1.17	0.3	28	47.76
Mollusks	3.01	3.97	0.67	0	16	15.74
Bioclasts	15.44	12.29	20.80	1	50.6	150.95
Lithoclasts	0.78	1.31	0.22	0	4	1.70
Intraclasts	0.45	1.36	0.23	0	6	1.86
Ooids	7.15	13.13	2.22	0	74	172.48
Micrite	31.24	15.05	2.54	0	63.6	226.61
<b>Lowstand:</b>						
Green algae	0.46	1.33	0.26	0	5	1.77
Red algae	0.57	1.33	0.26	0	6	1.76
Echinoderms	1.63	2.13	0.41	0	7	4.53
Rotaliids	0.60	1.03	0.20	0	3.3	1.05
Miliolids	0.13	0.34	0.07	0	1.5	0.12
Planktonic foraminifers	12.00	8.89	1.71	1	34	79.01
Mollusks	2.86	5.26	1.01	0	24	27.7
Bioclasts	30.60	18.43	3.55	6.9	63.6	339.74
Lithoclasts	1.21	2.89	0.56	0	12	8.38
Intraclasts	0.22	0.97	0.19	0	5	0.95
Ooids	2.23	3.98	0.77	0	17	15.81
Micrite	33.04	13.92	2.68	8.3	60	193.73

Note: SD = standard deviation, SE = standard error.

Table 11. Statistical description of turbidite deposits shed during sea-level highstand and lowstand, Site 1007.

	Mean	SD	SE	Minimum	Maximum	Variance
<b>Highstand:</b>						
Green algae	0.71	0.57	0.10	0	3	0.33
Red algae	0.45	0.97	0.18	0	3	0.95
Echinoderms	0.43	0.74	0.14	0	2.6	0.55
Rotaliids	0.46	0.65	0.12	0	2.6	0.43
Miliolids	0.03	0.09	0.02	0	0.3	0.01
Planktonic foraminifers	15.28	10.26	1.87	2	44.3	105.18
Mollusks	3.76	9.55	1.74	0	36	91.17
Bioclasts	22.71	11.32	2.07	0.5	52	128.10
Lithoclasts	0.11	0.28	0.05	0	1	0.08
Intraclasts	0.02	0.09	0.02	0	0.5	0.01
Ooids	0.82	1.55	0.28	0	7	2.41
Micrite	41.21	13.70	2.50	15	69	187.72
<b>Lowstand:</b>						
Green algae	0.01	0.06	0.01	0	0.3	0
Red algae	0.18	0.47	0.09	0	1.5	0.22
Echinoderms	0.53	0.86	0.16	0	3	0.73
Rotaliids	0.31	0.45	0.09	0	1.5	0.21
Miliolids	0.02	0.08	0.02	0	0.3	0.01
Planktonic foraminifers	18.01	13.12	2.52	2.6	55	172.01
Mollusks	7.29	14.4	2.77	0	46	207.33
Bioclasts	17.87	13.76	2.65	0.5	45	189.21
Lithoclasts	0.14	0.46	0.09	0	2.3	0.21
Intraclasts	0.19	0.68	0.13	0	3	0.46
Ooids	1.23	4.07	0.78	0	21	16.6
Micrite	44.16	16.55	3.18	14	70.3	273.75

Note: SD = standard deviation, SE = standard error.

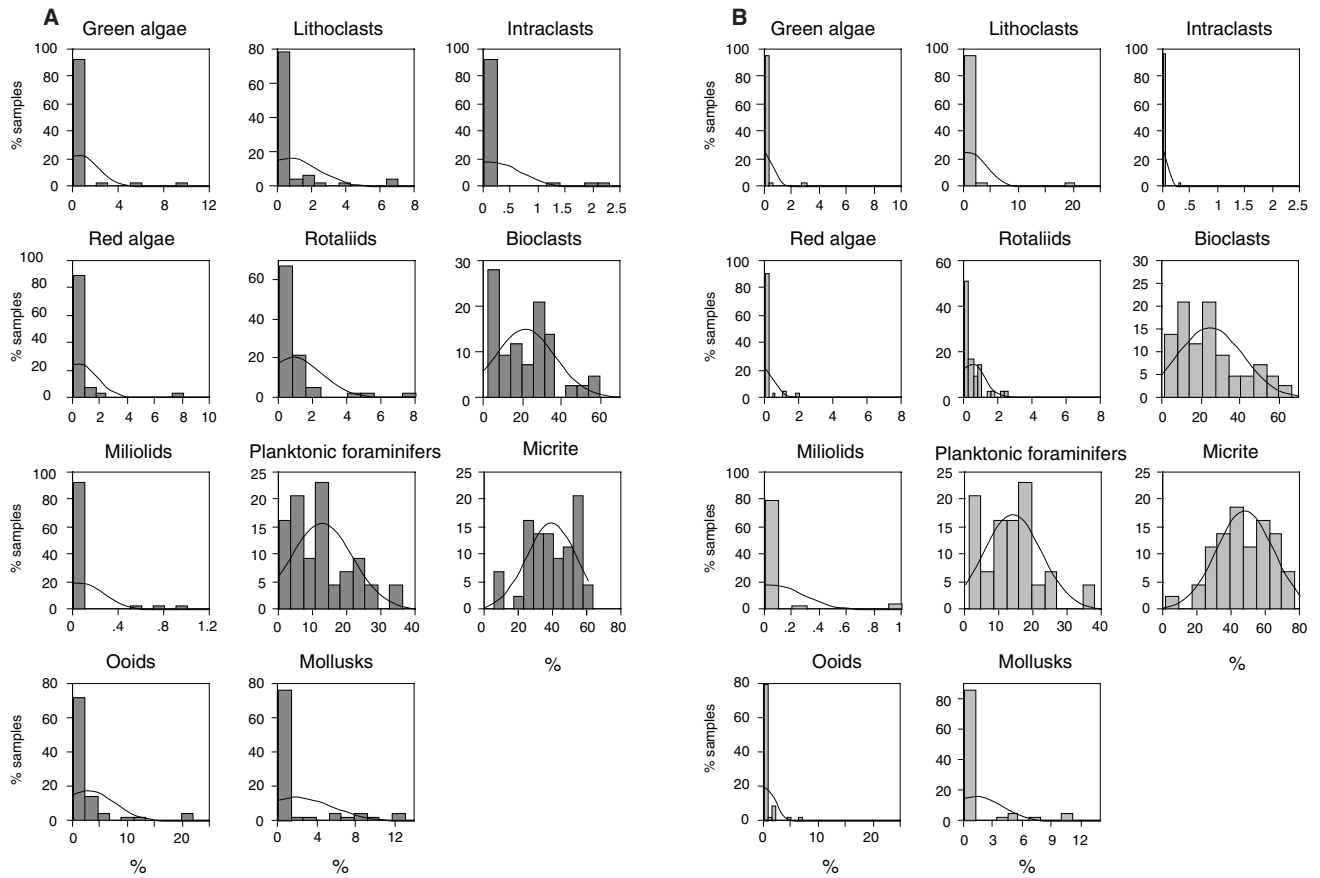


Figure 10. Comparison of the composition of background sediments deposited during (A) sea-level highstand and (B) sea-level lowstand at the lower slope (Site 1003; Miocene). The sediments deposited during high sea level show a higher abundance of shallow-water components including green and red algae, ooids, miliolids, and lithoclasts, but also rotaliids.

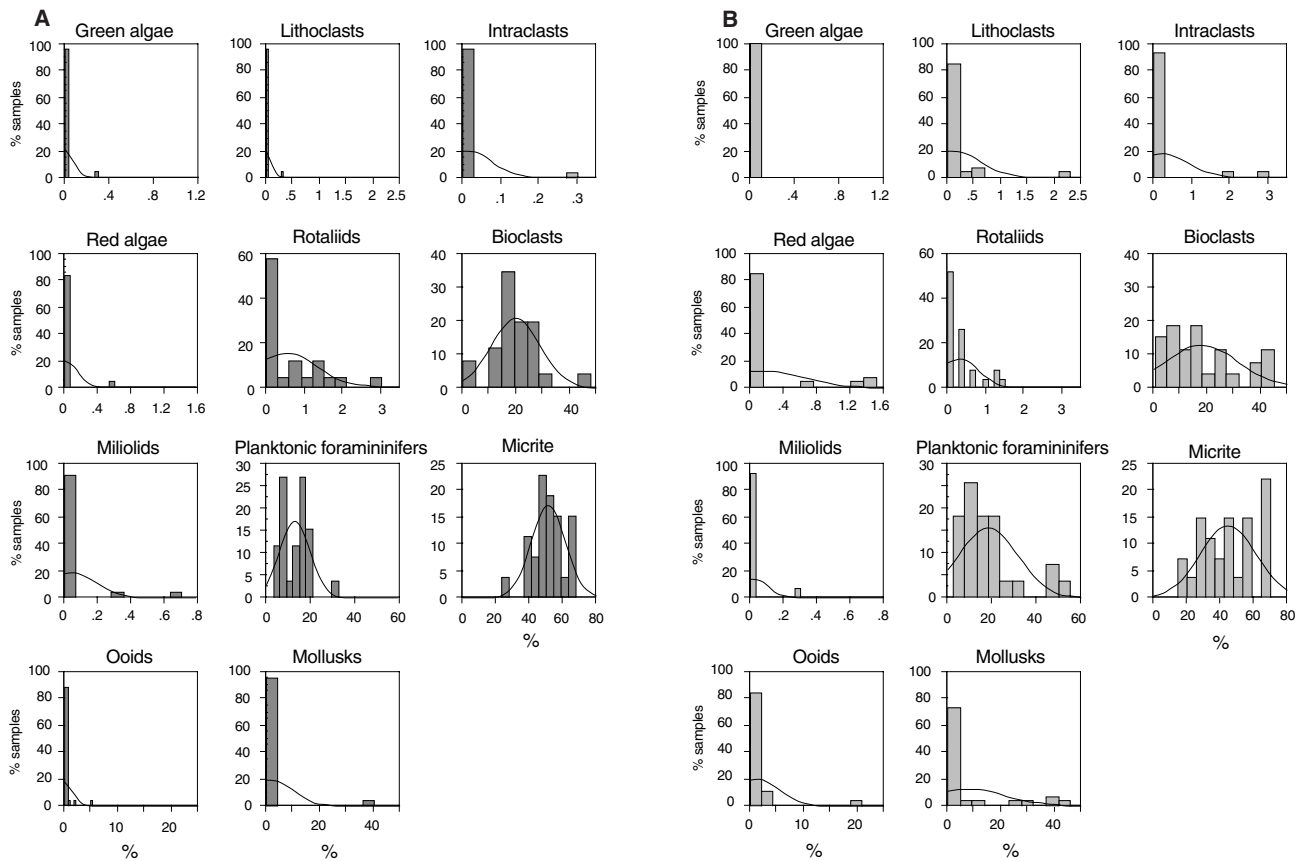


Figure 11. Distribution of background sediments deposited during (A) sea-level highstand and (B) sea-level lowstand in the basin (Site 1007; Miocene). Higher percentages of shallow-water components in the background sediments are deposited during sea-level lowstands (e.g. green algae, red algae, ooids, and lithoclasts).

Table 12. Statistical description of background sediments deposited during sea-level highstand and lowstand, Site 1003.

	Mean	SD	SE	Minimum	Maximum	Variance
<b>Highstand:</b>						
Green algae	0.41	1.71	0.26	0	10	2.91
Red algae	0.34	1.27	0.19	0	8	1.61
Echinoderms	1.08	2.04	0.31	0	10	4.18
Rotaliids	0.85	1.54	0.24	0	8	2.38
Miliolids	0.05	0.20	0.03	0	1	0.04
Planktonic foraminifers	12.39	9.04	1.38	0	36	81.77
Mollusks	1.85	3.69	0.56	0	13	13.61
Bioclasts	20.83	14.92	2.28	2.3	59	222.64
Lithoclasts	0.67	1.62	0.25	0	7	2.61
Intraclasts	0.13	0.49	0.08	0	2.3	0.24
Ooids	2.40	4.84	0.74	0	22	23.46
Micrite	38.37	14.53	2.22	0	63	211.07
<b>Lowstand:</b>						
Green algae	0.08	0.46	0.00	0	3	0.21
Red algae	0.10	0.37	0.00	0	2	0.14
Echinoderms	0.26	0.54	0.00	0	2	0.29
Rotaliids	0.44	0.63	0.00	0	2.6	0.4
Miliolids	0.05	0.21	0.00	0	1	0.05
Planktonic foraminifers	13.74	8.33	1.27	1	38	69.37
Mollusks	1.08	2.63	4.00	0	11	6.9
Bioclasts	24.08	16.74	2.55	1	66.3	280.37
Lithoclasts	0.67	3.14	0.48	0	20.3	9.86
Intraclasts	0.01	0.05	0.00	0	0.3	0.002
Ooids	0.47	1.32	0.20	0	7	1.76
Micrite	17.26	16.44	2.51	1.3	77	270.14

Note: SD = standard deviation, SE = standard error.

Table 13. Statistical description of background sediments deposited during sea-level highstand and lowstand, Site 1007.

	Mean	SD	SE	Minimum	Maximum	Variance
<b>Highstand:</b>						
Green algae	0.00	0.00	0.00	0	0	0.00
Red algae	0.02	0.12	0.02	0	0.6	0.01
Echinoderms	0.48	0.97	0.19	0	4	0.94
Rotaliids	0.53	0.79	0.15	0	3	0.62
Miliolids	0.04	0.15	0.03	0	0.7	0.02
Planktonic foraminifers	12.52	6.61	1.30	3	32.3	43.69
Mollusks	1.55	7.84	1.54	0	40	61.51
Bioclasts	19.61	9.15	1.97	0	48	83.67
Lithoclasts	0.01	0.06	0.01	0	0.3	0.00
Intraclasts	0.01	0.06	0.01	0	0.3	0.00
Ooids	0.35	1.07	0.21	0	5.3	1.15
Micrite	50.88	9.89	1.94	23	67.3	97.80
<b>Lowstand:</b>						
Green algae	0.01	0.06	0.01	0	0.3	0
Red algae	0.18	0.47	0.09	0	1.5	0.22
Echinoderms	0.53	0.86	0.16	0	3	0.73
Rotaliids	0.31	0.45	0.09	0	1.5	0.21
Miliolids	0.02	0.08	0.02	0	0.3	0.01
Planktonic foraminifers	18.01	13.12	2.52	2.6	55	172.01
Mollusks	7.29	14.4	2.77	0	46	207.33
Bioclasts	17.87	13.76	2.65	0.5	45	189.21
Lithoclasts	0.14	0.46	0.09	0	2.3	0.21
Intraclasts	0.19	0.68	0.13	0	3	0.46
Ooids	1.23	4.07	0.78	0	21	16.6
Micrite	44.16	16.55	3.18	14	70.3	273.75

Note: SD = standard deviation, SE = standard error.